DALTON
FULL PAPER

Synthesis and characterisation of manganese(II) compounds with tetradentate ligands based on the bispidine backbone

Peter Comba,*[a] Basil Kanellakopulos,[b] Charis Katsichtis,[a] Achim Lienke,[a] Hans Pritzkow[a] and Frank Rominger[c]

[a] *Anorganisch-Chemisches Institut der Universität Heidelberg, Im Neuenheimer Feld 270, 69120 Heidelberg, Germany. E-mail: comba@akcomba.oci.uni-heidelberg.de. Fax: ++49-6221-546617*

[b] *Forschungszentrum Karlsruhe, Institut für Technische Chemie, Postfach 3640, 76021 Karlsruhe, Germany*

[c] *Organisch-Chemisches Institut der Universität Heidelberg, Im Neuenheimer Feld 270, 69120 Heidelberg, Germany*

Received 29th July 1998, Accepted 2nd October 1998

Reaction of the tetradentate ligand dimethyl 3,7-dimethyl-9-oxo-2,4-bis(2-pyridyl)-3,7-diazabicyclo[3.3.1]nonane-1,5-dicarboxylate (L^1) with manganese(II) chloride or iodide in methanol yielded [MnL^1Cl_2] and [MnL^1I_2], respectively. Reaction with silver(I) triflate $Ag(O_3SCF_3)$ converted these compounds into [$MnL^1(O_3SCF_3)_2$]. Reduction of L^1 with $NaBH_4$ in MeOH and $LiAlH_4$ in THF led to the triol 1,5-bis(hydroxymethylene)-3,7-dimethyl-2,4-bis(2-pyridyl)-3,7-diazabicyclo[3.3.1]nonan-9-ol (L^2); the reduction is stereoselective and yields the *syn* isomer. Complexation of manganese(II) chloride and iodide with L^2 produced [MnL^2Cl_2] and [MnL^2I_2] and these have a higher thermal stability than [MnL^1X_2]. The complexes [MnL^1Cl_2], [MnL^1I_2], [$MnL^1(O_3SCF_3)_2$], [MnL^2Cl_2] and [MnL^2I_2] are characterised spectroscopically, electrochemically and by their magnetic, conductometric, thermal and structural properties (X-ray analyses of [MnL^1Cl_2] and [MnL^2Cl_2]).

Introduction

Manganese is an essential element in aerobic organisms. As part of several enzymatic systems it is directly involved in various processes of oxygen metabolism. Important examples are the conversion of two water molecules into oxygen (photosynthesis), catalysed by multinuclear manganese clusters,[1,2] and the disproportionation of two superoxide ions to hydrogen peroxide and oxygen, a process catalysed by a mononuclear manganese enzyme (Mn-SOD).[2–4] In addition to the formation and activation of oxygen, manganese compounds are used in industrial processes as stabilisers, for example in combination with halides.[5] Rigid tetradentate ligands may produce relatively inert complex fragments with one or two sites, where small substrates can be bound and activated. Among others, these fragments might be used to scavenge and deactivate radicals such as hydroperoxo which are believed to be responsible for the thermooxidative yellowing of aliphatic polyamides.[6] Here manganese(II) compounds of the substituted bispidine type ligands L^1 {dimethyl 3,7-dimethyl-9-oxo-2,4-bis(2-pyridyl)-3,7-diazabicyclo[3.3.1]nonane-1,5-dicarboxylate} and L^2 {1,5-bis(hydroxymethylene)-3,7-dimethyl-2,4-bis(2-pyridyl)-3,7-diazabicyclo[3.3.1]nonan-9-ol} (Chart 1) have been prepared and characterised and the influence of various anions (Cl^-, I^-, $CF_3SO_3^-$) on their solid state and solution properties have been studied in detail.

Crystal structures[7,8] and solution NMR studies[8–11] of several substituted bispidines indicate that the backbone favors a flattened chair/chair conformation with substituents (such as the pyridyl groups in L^1 and L^2) in equatorial positions. Compounds L^1 and L^2 have a bowl-like structure (Chart 1) which leaves one or two vacant co-ordination sites on the metal of ML^1 and ML^2 fragments, and this is of interest for catalytic applications.

Substituted dimethyl 1,5-dicarboxylates of type L^1 have a limited stability at high temperatures and in strong acidic or alkaline media, retro-Mannich reactions and decarboxylation being the most important degradation reactions. Reduction of all carbonyl groups might lead to a considerable stabilisation but treatment with $LiAlH_4$ is known to produce hygroscopic materials which are difficult to purify.[9] We also present the first successful synthesis of a fully reduced substituted bispidine type ligand L^2 (see Chart 1).

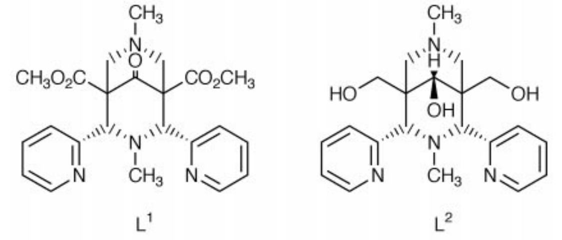

L^1 L^2

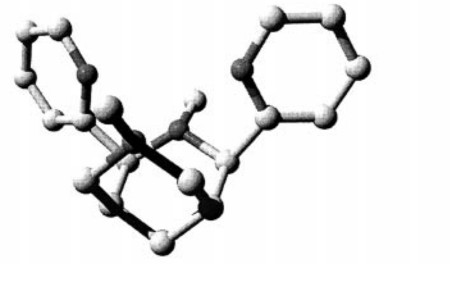

Experimental

Physical methods

Proton and ^{13}C NMR spectra at 200.13 or 300.13 and 50.32 or 75.47 MHz, respectively, were measured with Bruker AS 200 or WH 300 instruments, with dichloromethane as internal reference, infrared spectra (KBr pellets) with a Perkin-Elmer

16PC FT-IR or FTR2000 instrument, electronic spectra with a Perkin-Elmer Lambda 19 instrument. Variable temperature and variable magnetic field measurements were made with a Bruker Faraday balance. Cyclic voltammograms were recorded on a BAS 100B system, using 1×10^{-3} mol dm^{-3} solutions of the manganese compounds in acetonitrile (0.1 mol dm^{-3} n-Bu$_4$NClO$_4$), at a glassy carbon electrode with a Ag–AgNO$_3$ reference electrode and a platinum wire as the auxiliary electrode; the results were independent of the scan rate in the range 0.02–0.2 V s^{-1}. Conductivity data for 1×10^{-3} mol dm^{-3} acetonitrile solutions of the manganese compounds at 298 K were measured with a Knick 703 conductivity bridge. Thermogravimetric data were obtained with a SEIKO TG/DTA 6200 or a Perkin-Elmer TGA 7 instrument. Mass spectra (FAB) were measured with a Finnigan 8400 instrument, using a 3-nitrobenzyl alcohol matrix. Elemental analyses were performed by the microanalytical laboratory of the chemical institutes of the University of Heidelberg.

Structure determinations

Crystal data. [MnL^{1}Cl$_2$], C$_{23}$H$_{26}$Cl$_2$MnN$_4$O$_5$·C$_2$H$_6$O, triclinic, space group $P\bar{1}$, $a = 11.577(6)$, $b = 11.812(6)$, $c = 11.951(6)$ Å, $\alpha = 110.71(3)$, $\beta = 102.50(3)$, $\gamma = 105.15(3)$°, $V = 1386.5(12)$ Å^3, $Z = 2$, $D_c = 1.48$ g cm^{-3}, $F(000) = 634$, $\mu = 0.716$ mm^{-1}, crystal size $0.15 \times 0.20 \times 0.35$ mm.

Intensity data were collected at 203(2) K with a Siemens-Stoe AED2 diffractometer (Mo-Kα radiation, $\lambda = 0.71073$ Å, ω scan) up to $2\theta = 50°$ [4443 unique reflections, 3133 observed with $I > 2\sigma(I)$]. Data were corrected for Lorentz-polarisation and absorption effects (ψ scan, transmission range 0.95–1.00). The structure was solved by direct methods (SHELXS 86[12a]). The refinement was based on F^2 with all measured reflections (SHELXL 97[12b]). The cell contains a disordered solvent molecule, which could not be modeled successfully. The non-hydrogen atoms were refined anisotropically. Hydrogen atoms bound directly to the heterocycle were located in a Fourier-difference map and refined isotropically. All other hydrogen atoms were inserted in calculated positions or as part of a rigid group (methyl) and only common isotropic thermal parameters were refined. The refinement (367 parameters) converged at $R1 = 0.052$ (observed reflections only) and $wR2 = 0.141$ (all reflections); goodness of fit = 1.062.

[MnL^{2}Cl$_2$], C$_{21}$H$_{28}$Cl$_2$MnN$_4$O$_3$, monoclinic, space group $C2/c$, $a = 33.556(9)$, $b = 9.476(3)$, $c = 31.444(9)$ Å, $\beta = 109.62(10)$°, $V = 9418.3(5)$ Å^3, $Z = 16$, $D_c = 1.40$ g cm^{-3}, $F(000) = 4416$, $\mu = 0.82$ mm^{-1}, crystal size $0.19 \times 0.10 \times 0.09$ mm.

34438 (8197 unique) Reflections were collected at 200 K on a Siemens SMART CCD diffractometer employing graphite-monochromated Mo-Kα radiation; 0.3° ω scans, data reduction including Lorentz-polarisation and absorption corrections (empirical) were carried out. The structure was solved by direct methods with SHELXTL PLUS;[13] the hydrogen atoms were included at calculated sites with isotropic thermal parameters derived from the atoms to which they are connected. The refinement[12b] (full-matrix least-squares methods) of 623 variables against 8197 reflections converged at $R1 = 0.062$ and $wR2 = 0.108$; residual electron density 0.51 and −0.44 e Å^{-3}; goodness of fit = 1.09. The second independent molecule contains two disordered OH groups. The C–O distance in these groups was fixed at an appropriate value (1.426 Å with a standard deviation of 0.03). The two positions of the O atoms were refined with coupled occupation factors (adding up to 1.00). The crystal also contains one disordered solvent molecule per asymmetric unit, probably EtOH or Et$_2$O, which could not be modeled successfully.

Selected bond distances and valence angles are given in Table 1; atom labeling schemes are defined in Fig. 1 which are ORTEP[14] diagrams of the experimental structures.

CCDC reference number 186/1189.

See http://www.rsc.org/suppdata/dt/1998/3997/ for crystallographic files in .cif format.

Syntheses

L^1. Compound L^1 was prepared as decribed in the literature.[15,16] Yield 67%, mp 184 °C (Found: C, 62.9; H, 6.0; N, 12.7. Calc. for C$_{23}$H$_{26}$N$_4$O$_5$: C, 63.1; H, 6.0; N, 12.8%). NMR (CD$_2$Cl$_2$, 25 °C): ^{1}H (200 MHz), δ 2.0 (s, 3 H, N^7–CH$_3$), 2.22 (s, 3 H, N^3–CH$_3$), 2.45 (d, $^2J = 12$, 2 H, H6$_{ax}$, H8$_{ax}$), 2.93 (d, $^2J = 12$, 2 H, H6$_{eq}$, H8$_{eq}$), 3.75 (s, 6 H, OCH$_3$), 4.67 (s, 2 H, H2, H4), 7.23 (ddd, $^3J_o = 7.6$, $^3J_{o'} = 4.7$, $^4J_m = 1.1$, 2 H, py H5), 7.80 (td, $^3J_o = 7.6$, $^4J_m = 1.8$, 2 H, py H4), 8.07 (d, $^3J_o = 7.6$, 2 H, py H3) and 8.49 (d, $^3J_{o'} = 4.7$ Hz, 2 H, py H6); ^{13}C (50 MHz), δ 43.0 (N^7–CH$_3$), 44.2 (N^3–CH$_3$), 52.2 (OCH$_3$), 60.8 (C6, C8), 62.4 (C2, C4), 73.8 (C1, C5), 122.9 (py C5), 123.6 (py C3), 136.4 (py C4), 149.1 (py C6), 159.1 (py C2), 168.5 (CO ester) and 203.6 (C9). IR (KBr): $\tilde{\nu}$/cm^{-1} >3000w (C$_{py}$–H), 2953s (CH$_2$), 2897w (CH), 2859m (OC–H), 2789m (NC–H, Bohlmann), 1737s (C=O, ester and ketone), 1593s (ν-8a, py), 1423s (CH$_2$), 1293, 1277s (C–OCH$_3$) and 759m (C$_{ar}$–H, 4 H neighboring).

L^2·2MeOH. Sodium tetrahydroborate (6.47 g, 0.171 mol) was added slowly to a cooled suspension of L^1 (7.5 g, 17.10 mmol) in 250 ml absolute methanol; the temperature remained below 0 °C. After stirring at room temperature for 12 h the solvent was removed under reduced pressure. The solid product was dissolved in water (400 ml), and the solution stirred for 2 h. The white suspension was extracted with CHCl$_3$ (400 ml), the solvent removed and the solid stirred in hydrochloric acid (10%, 200 ml) for 1 h. After neutralisation with NaOH and extraction with CHCl$_3$ (400 ml), the organic phase was dried over magnesium sulfate; removal of solvent under reduced pressure produced a white solid. Yield: 4.2 g of the crude product mixture. To a solution of this product (4.2 g) in absolute THF (150 ml) was added dropwise a filtered solution of LiAlH$_4$ (1.55 g, 40.8 mmol) in absolute THF (41 ml). After stirring for 12 h at room temperature the resulting yellow solution was treated with an aqueous solution of sodium tartrate. The two layers were separated and the aqueous phase extracted with chloroform (100 ml). The organic phases were collected and the same volume of chloroform was added. The water phase was removed and the organic phase dried over magnesium sulfate. Removal of the solvent under reduced pressure and recrystallisation from ethanol–methanol yielded white crystals: 2.48 g (6.45 mmol, 35%) (Found: C, 61.1; H, 7.4; N, 12.1. Calc. for C$_{23}$H$_{36}$N$_4$O$_5$: C, 61.6; H, 8.0; N, 12.4%), mp 74–75 °C. NMR (CD$_2$Cl$_2$, 25 °C): ^{1}H (300 MHz), δ 1.37 (d, $^2J = 12$, 2 H, H6$_{ax}$, H8$_{ax}$), 1.87 (s, 3 H, N^7–CH$_3$), 2.05 (s, 3 H, N^3–CH$_3$), 2.18 (d, $^2J = 12$, 2 H, H6$_{eq}$, H8$_{eq}$), 3.16 (d, $^2J = 12.1$, 2 H, H10, H11), 3.40 (d, $^2J = 12.1$, 2 H, H10, H11), 3.55–3.76 (m, 2 H, CH$_2$O*H*), 3.85 (s, 1 H, H9), 4.08 (s, 1 H, C9–OH), 4.25 (s, 2 H, H2, H4), 7.22 (ddd, $^3J_o = 7.3$, $^3J_{o'} = 4.9$, $^4J_m = 1.3$, 2 H, py H5), 7.78 (td, $^3J_o = 7.8$, $^4J_m = 1.6$, 2 H, py H4), 8.14 (d, $^3J_o = 8.0$, 2 H, py H3) and 8.46 (d, $^3J_{o'} = 4.8$ Hz, 2 H, py H6); ^{13}C (75 MHz), δ 42.9 (N^7–CH$_3$), 44.5 (N^3–CH$_3$), 58.1 (C6, C8), 68.2 (C2, C4), 68.6 (C10, C11), 73.5 (C1, C5), 81.1 (C9), 122.6 (py C5), 124.4 (py C3), 137.0 (py C4), 148.4 (py C6) and 163.4 (py C2). IR (KBr): $\tilde{\nu}$/cm^{-1} >3000w (C$_{py}$–H), 2932m (CH$_2$), 2849w (CH), 2791w (NC–H, Bohlmann), 1592s (ν-8a, py), 1086, 1064 (C–OH) and 759m (C$_{ar}$–H, 4 H neighboring). Mass spectral analysis showed the [M + H]$^+$ ion at m/z 385.

[MnL^{1}Cl$_2$]. A solution of MnCl$_2$·4H$_2$O (67 mg, 0.34 mmol) in methanol (4 ml) was added to a hot solution of L^1 (150 mg, 0.34 mmol) in methanol (5 ml). This was refluxed for 15 min and stored overnight at 5 °C. The yellow precipitate was filtered off, washed with cold ethanol, recrystallised from ethanol–methanol and vacuum dried. Yield: 0.16 g (0.28 mmol, 84%) (Found: C, 48.0; H, 5.0; N, 9.5. Calc. for C$_{23}$H$_{26}$Cl$_2$MnN$_4$O$_5$·0.6

H_2O: C, 48.0; H, 4.8; N, 9.7%). IR (KBr): $\tilde{\nu}$/cm^{-1} >3000m (C_{py}–H), 2968w (CH_2), 2944w (CH), 2826w (OC–H), 1724s (C=O), 1603m (ν-8a, py), 1442s (CH_2), 1272, 1252s (C–OCH_3) and 780m (C_{ar}–H, 4 H neighboring). Magnetic moment (20 °C) = 5.94 ± 0.05 μ_B. Electric conductivity (25 °C, CH_3CN): $\Lambda_M = 25\ \Omega^{-1}\ cm^2\ mol^{-1}$. CV: E_0 = 0.568 V (*vs.* Ag–$AgNO_3$).

[MnL^{1}I$_2$]. Manganese(II) iodide (105 mg, 0.34 mmol) was added to a hot solution of L^1 (150 mg, 0.34 mmol) in methanol (10 ml). After refluxing the suspension for 5 h the solution was filtered. Removal of the solvent from the deep yellow solution and recrystallisation of the resulting solid from ethanol yielded a pale brown product. Yield: 0.13 g (0.17 mmol, 51%) (Found: C, 37.0; H, 4.0; N, 7.2. Calc. for $C_{23}H_{26}I_2MnN_4O_5$: C, 37.0; H, 3.5; N, 7.5%). IR (KBr): $\tilde{\nu}$/cm^{-1} > 3000m (C_{py}–H), 2948w (CH_2), 2899w (CH), 2834w (O–CH), 1733s (C=O), 1601m (ν-8a, py), 1444s (CH_2), 1265, 1216s (C–OCH_3), 779m (C_{ar}–H, 4 H neighboring). Magnetic moment (20 °C) = 5.89 ± 0.05 μ_B. Electric conductivity (25 °C, CH_3CN): $\Lambda_M = 139\ \Omega^{-1}\ cm^2\ mol^{-1}$.

[MnL^1(O$_3$SCF$_3$)$_2$]. Silver triflate (0.228 g, 0.89 mmol) was added to a solution of [MnL^{1}Cl$_2$] (0.25 g, 0.45 mmol) in CH_3CN (120 ml) and methanol (3 ml). After stirring overnight the white precipitate was filtered off and the solvent removed. The resulting white solid was recrystallised from CH_3CN–diethyl ether and dried *in vacuo*. Yield: 0.30 g (0.38 mmol, 84%) (Found: C, 37.5; H, 3.9; N, 6.7. Calc. for $C_{25}H_{26}F_6MnN_4O_{11}S_2$: C, 37.9; H, 3.3; N, 7.1%). IR (KBr): $\tilde{\nu}$/cm^{-1} >3000s (C_{py}–H), 2960m (CH_2), 2928w (CH), 1741s (C=O), 1605m (ν-8a, py), 1449s (CH_2), 1288, 1030 (SO_3), 1242, 1167 (CF_3). Magnetic moment (25 °C) = 5.52 ± 0.2 μ_B. Electric conductivity (25 °C, CH_3CN): $\Lambda_M = 228\ \Omega^{-1}\ cm^2\ mol^{-1}$.

[MnL^{2}Cl$_2$]·0.5H$_2$O. A solution of $MnCl_2 \cdot 4H_2O$ (0.618 g, 3.121 mmol) in methanol (10 ml) was added to a hot solution of L^2 (1.2 g, 3.121 mmol) in methanol (10 ml). Refluxing for 15 min and removing the solvent by rotatory evaporation yielded an orange powder, which was recrystallised from ethanol and dried *in vacuo*. Yield: 1.2 g (2.37 mmol, 76%) Found: C, 48.5; H, 6.0; N, 10.0. Calc. for $C_{21}H_{29}Cl_2MnN_4O_{3.5}$: C, 48.6; H, 5.6; N, 10.8%). IR (KBr): $\tilde{\nu}$/cm^{-1} >3000s (C_{py}–H), 2957w (CH_2), 2884m (CH), 1602s (ν-8a, py), 1444s (CH_2), 1048s (C–OH) and 778s (C_{ar}–H, 4 H neighboring). Magnetic moment (25 °C) = 5.77 ± 0.05 μ_B. Electric conductivity (25 °C, CH_3CN): $\Lambda_M = 22\ \Omega^{-1}\ cm^2\ mol^{-1}$. CV: E_0 = 0.513 V (*vs.* Ag–$AgNO_3$).

[MnL^{2}I$_2$]. Manganese(II) iodide (0.602 g, 1.95 mmol) was added to a hot solution of L^2 (0.75 g, 1.95 mmol) in methanol (40 ml). After refluxing for 5 h the insoluble solid was filtered off. Removing of the solvent from the deep brown solution and recrystallisation from ethanol yielded a pale brown powder, which was dried *in vacuo*. Yield: 1.18 g [1.70 mmol, 87%; despite numerous recrystallisations from ethanol the product was always contaminated with metal-free ligand (elemental analysis, IR spectra)]. IR (KBr): $\tilde{\nu}$/cm^{-1} >3000s (C_{py}–H), 2930m (CH_2), 2875m (CH), 1602m (ν-8a, py, complex), 1591m (ν-8a, py, free L^2), 1472m (CH_2), 1043s (C–OH) and 772m (C_{ar}–H, 4 H neighboring). Electric conductivity (25 °C, CH_3CN): $\Lambda_M = 119\ \Omega^{-1}\ cm^2\ mol^{-1}$. A cyclic voltammogram in CH_3CN showed the presence of free iodide in solution (see also Results and discussion).

Results and discussion

Syntheses

Compound L^1 was prepared in high yield by a double Mannich condensation.[15,16] The reduction of L^1 with $NaBH_4$ did not yield the *syn*-dimethyl 9-ol 1,5-dicarboxylate[9] but a mixture of the desired product and compounds with one or two ester substituents reduced to alcohols, the main product being a diol. Reaction of this mixture with an excess of lithium aluminium hydride in THF and removal of aluminium(III) by complexation with tartrate yielded the new ligand L^2 in fair yields. Compound L^1 could also be directly reduced with lithium aluminium hydride but this produced a mixture of L^2 and the corresponding 9-*anti* isomer. This could not be separated by recrystallisation or flash chromatography. Reaction of the chloride or iodide salts of manganese(II) with L^1 or L^2 in hot methanol produced [MnL^{1}Cl$_2$], [MnL^{1}I$_2$], [MnL^{2}Cl$_2$] and [MnL^{2}I$_2$]; [MnL^1(SO$_3$CF$_3$)$_2$] was obtained from [MnL^{1}Cl$_2$] and silver triflate in acetonitrile–methanol. Owing to the low solubility of MnI_2 in methanol the yields of [MnL^{1}I$_2$] and [MnL^{2}I$_2$] were rather small and the products difficult to separate from unchanged starting material.

Crystal structures

X-Ray quality crystals were obtained by vapor diffusion of diethyl ether into methanolic solutions of the complexes. The ORTEP[14] plots of the experimentally determined structures are presented in Fig. 1 and selected structural parameters in Table 1. In the asymmetric unit of [MnL^{2}Cl$_2$] there are two independent molecules; both have similar structural properties. The manganese(II) center in all three structures ([MnL^{1}Cl$_2$] and both independent molecules of [MnL^{2}Cl$_2$]) has an approximately *cis*-octahedral geometry, with the two pyridyl-N donors

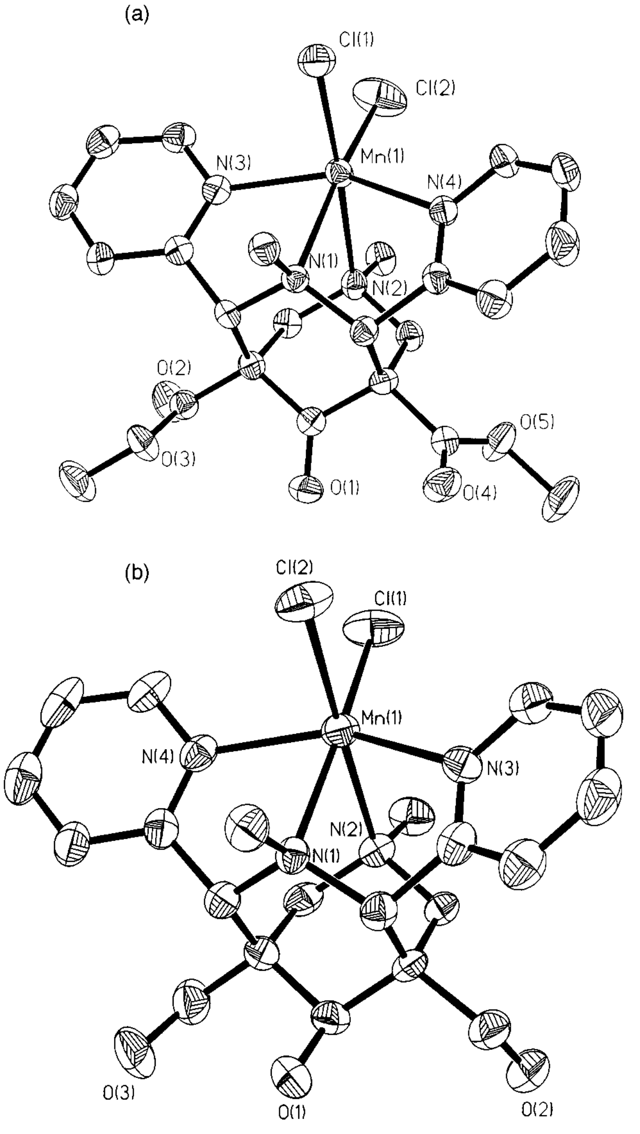

Fig. 1 The ORTEP[14] plots with the numbering scheme of (a) [MnL^{1}Cl$_2$] and (b) [MnL^{2}Cl$_2$] (hydrogen atoms are omitted for clarity).

Table 1 Selected structural parameters (bond lengths in Å, angles in °) of $[\mathrm{MnL^1Cl_2}]$ and $[\mathrm{MnL^2Cl_2}]$

	$[\mathrm{MnL^1Cl_2}]$	$[\mathrm{MnL^2Cl_2}]$[a]	
Mn(1)–N(1)	2.388(4)	2.346(4)	2.343(4)
Mn(1)–N(2)	2.531(4)	2.437(5)	2.446(5)
Mn(1)–N(3)	2.231(4)	2.232(5)	2.217(4)
Mn(1)–N(4)	2.255(4)	2.232(5)	2.241(4)
Mn(1)–Cl(1)	2.462(2)	2.434(2)	2.395(2)
Mn(1)–Cl(2)	2.404(2)	2.530(2)	2.523(3)
N(2)–Mn(1)–N(1)	74.0(1)	77.2(2)	76.9(2)
N(3)–Mn(1)–N(4)	144.4(1)	146.2(2)	147.4(2)
N(1)–Mn(1)–N(4)	72.2(1)	72.6(2)	74.1(2)
N(2)–Mn(1)–N(3)	85.5(1)	88.0(2)	88.1(2)

[a] The asymmetric unit of $[\mathrm{MnL^2Cl_2}]$ contains two independent molecules. For the numbering of the second molecule 30 has to be added to the atom numbers of the first molecule.

Table 2 Characteristic IR transitions ($\mathrm{cm^{-1}}$) for $\mathrm{L^1}$ and $\mathrm{L^2}$ and the corresponding manganese(II) compounds

Compound	$\mathrm{C_{pyridine}–N_{pyridine}}$	$\mathrm{RNCH_3}$	$\tilde{\nu}_{\mathrm{complex}} - \tilde{\nu}_{\mathrm{L}}$
$\mathrm{L^1}$	1587	2796	—
$\mathrm{L^2}$	1592	2790	—
$[\mathrm{MnL^1Cl_2}]$	1603	—	16
$[\mathrm{MnL^1I_2}]$	1601	—	14
$[\mathrm{MnL^1(O_3SCF_3)_2}]$	1605	—	18
$[\mathrm{MnL^2Cl_2}]$	1602	—	10
$[\mathrm{MnL^2I_2}]$	1601	—	9

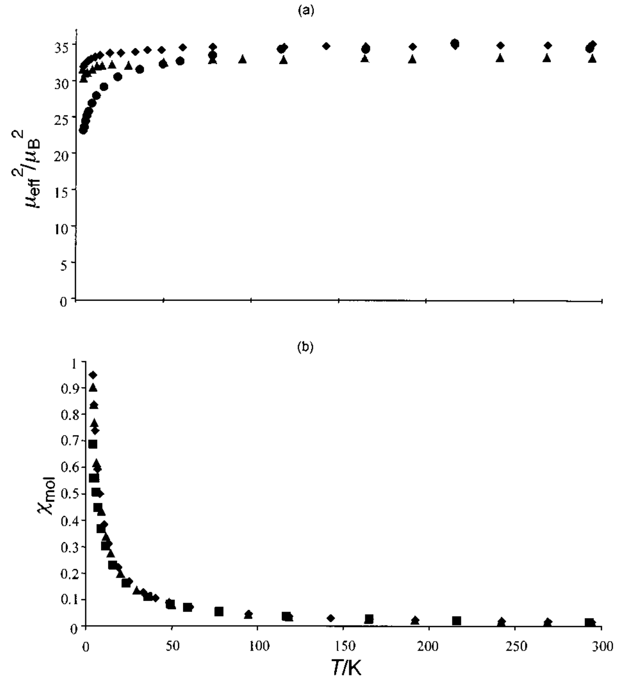

Fig. 2 The temperature dependence of (a) the square of the effective magnetic moment and (b) the magnetic susceptibility of $[\mathrm{MnL^1Cl_2}]$ (◆), $[\mathrm{MnL^1I_2}]$ (●) and $[\mathrm{MnL^2Cl_2}]$ (▲).

in axial sites. Owing to the rigidity of the bispidine-type backbone the main mode of distortion from octahedral geometry is the $\mathrm{N_{py}}$–Mn–$\mathrm{N_{py}}$ (*trans*) angle which is compressed to approximately 140–150° {144.4(1)° in $[\mathrm{MnL^1Cl_2}]$ and 146.2(2)° in $[\mathrm{MnL^2Cl_2}]$}. The cobalt(II) complex of $\mathrm{L^1}$[17] and the manganese(II) complex of bipyridine[18] also adopt *cis*-octahedral geometries and have *trans* angles of 149.8(3) and 152.2(1)°, respectively. A recently isolated and structurally characterised $[\mathrm{CuL^1Cl}]^+$ cation has a distorted square pyramidal chromophore with one of the amine donors (unsubstituted six-membered ring) in the axial position.[19] There are two distinct sets of Mn–N bond distances in $[\mathrm{MnL^1Cl_2}]$ and $[\mathrm{MnL^2Cl_2}]$. On average, the Mn–$\mathrm{N_{pyridine}}$ distances are 2.24 Å, the Mn–$\mathrm{N_{amine}}$ distances 2.43 Å. These are as expected from other manganese(II) compounds with pyridine and amine donors.[18,20] Interestingly, in both structures the Mn–N distances to the amine donor of the substituted six-membered ring are significantly shorter than those to the amine of the unsubstituted ring {$[\mathrm{MnL^1Cl_2}]$: 2.388(4) *vs.* 2.531(4) Å; $[\mathrm{MnL^2Cl_2}]$: 2.346(4) *vs.* 2.437(5) Å}. The same observation was made with the corresponding cobalt(II) compound, for which an experimental and a computed structure were reported.[17] In the copper(II) compound cited above the elongation of the axial bond to one of the amine donors is increased by a Jahn–Teller distortion.[19] It emerges that this distortion mode is the result of the rigid geometry of the substituted bispidine backbone.

Solid state properties

Infrared spectroscopy was used to confirm complexation of $\mathrm{L^1}$ and $\mathrm{L^2}$ to manganese(II). The ligands and complexes have two characteristic bands, $\nu_{\mathrm{C=N}}$ (pyridine) and $\nu_{\mathrm{N–C}}$ (Bohlmann), see Table 2.[15,16,21,22] The pyridine stretching mode at approximately 1600 $\mathrm{cm^{-1}}$[15,16] is shifted to higher energy upon co-ordination to manganese(II) (approximately 10–15 $\mathrm{cm^{-1}}$). The Bohlmann band at approximately 2800 $\mathrm{cm^{-1}}$ occurs when the free electron pair of the amine donor is anticoplanar to a CH group.[16,21,22] Upon complexation this band disappears.

The room temperature magnetic moments of $[\mathrm{MnL^1Cl_2}]$, $[\mathrm{MnL^1I_2}]$, $[\mathrm{MnL^1(O_3SCF_3)_2}]$ and $[\mathrm{MnL^2Cl_2}]$ are 5.94 ± 0.05, 5.89 ± 0.05, 5.52 ± 0.2 and 5.77 ± 0.05 μ_{B}, respectively (the value for $[\mathrm{MnL^2I_2}]$ is not reported due to problems with the purification, see Experimental section). These magnetic moments are close to the value of 5.92 μ_{B}, expected for a high-spin $\mathrm{d^5}$ ion ($^6\mathrm{A_{1g}}$ ground term) in an octahedral environment (spin-only value).

The values of μ_{eff}^2 for the chloro complexes remain nearly constant with temperature {see Fig. 2; μ_{eff} (4.2 K) = 5.65 μ_{B} or 5.51 μ_{B} for $[\mathrm{MnL^1Cl_2}]$ and $[\mathrm{MnL^2Cl_2}]$, respectively}. A small decrease at low temperature has been observed for other octahedral manganese(II) compounds.[22] For $[\mathrm{MnL^1I_2}]$ the value of μ_{eff}^2 decreases significantly below 100 K [μ_{eff} (4.2 K) = 4.80 μ_{B}]. This may be due to a distortion of the co-ordination geometry and a concomitant decrease of the ligand field strength.

The thermal stability of $[\mathrm{MnL^1Cl_2}]$, $[\mathrm{MnL^1I_2}]$, $[\mathrm{MnL^2Cl_2}]$ and $[\mathrm{MnL^2I_2}]$ was determined by thermogravimetric analyses. Thermal decomposition of the complexes of $\mathrm{L^1}$ starts at temperatures around 200 °C ($[\mathrm{MnL^1Cl_2}]$, 227 $[\mathrm{MnL^1I_2}]$, 212 °C). Based on the weight loss ($[\mathrm{MnL^1Cl_2}]$, 21; $[\mathrm{MnL^2I_2}]$, 8%) this may be due to the loss of two or one ester substituents, respectively. If the product of the thermal decomposition process of the chloro compound is heated again in a second cycle on the thermobalance the decomposition temperature increases significantly from 227 to 295 °C. The latter value is close to the decomposition temperature of $[\mathrm{MnL^2Cl_2}]$ (327 °C). This is further support for the interpretation that the first decomposition (227 °C) is due to decarboxylation of the ester substituents.

Solution properties

Electrochemical, conductivity and electronic spectroscopic data were obtained from acetonitrile solutions. The electronic spectra are dominated by the expected spin-forbidden transitions of octahedral manganese(II) chromophores and charge transfer transitions at relatively low energy due to the pyridine donors ($\tilde{\nu}/\mathrm{cm^{-1}}$: $[\mathrm{MnL^1Cl_2}]$, 20170, 25980, 29190, 31470, 38080; $[\mathrm{MnL^1I_2}]$, 18150, 23000, 26450, 32140, 38100). A full assignment of the d–d spectrum was not appropriate since these transitions are not much affected by the donors. The observation that the solution electronic spectra of $[\mathrm{MnL^1Cl_2}]$ and

$[MnL^2Cl_2]$ are identical to the corresponding solid state spectra while for the iodo complexes there are small but significant differences indicates that for the chloro complexes the solid state structures are retained in solution. This also emerges from the electrochemical and conductivity data (see below). The fact that the spectroscopic differences for the iodo complexes are only marginal indicates that octahedral co-ordination is retained. The observation of free iodide (electrochemistry) and of a 1 : 1 electrolyte (conductivity measurements) indicates that there is some ligand exchange.

Cyclic voltammetry indicates that there is a considerable difference between the chloro and the iodo compounds. The behaviour of the complexes of L^1 and L^2 is very similar. For the iodo compounds $[MnL^1I_2]$ and $[MnL^2I_2]$ free iodide prevents the observation of a Mn^{II}–Mn^{III} couple. This indicates that, in acetonitrile, there is ligand exchange that produces octahedral mono- or bis-acetonitrile compounds and free iodide. For $[MnL^1Cl_2]$ and $[MnL^2Cl_2]$ there are reversible oxidation waves [$E_0(Mn^{II}–Mn^{III}) = 0.568$ and 0.513 V for the complexes of L^1 and L^2, respectively], and the absence of free chloride indicates that there is no ligand exchange in these cases. This is confirmed by the electronic spectroscopic data (see above). The reduced form (Mn^{II}) is slightly more stable for L^1 than for L^2.

Further information on the structures present in solution emerges from the electric conductivity data [see Experimental section; the conductivities of n-Bu_4NI and $Fe(O_3SCF_3)_2$ are 153 and 196 Ω^{-1} cm^2 mol^{-1}, respectively). The chloro compounds $[MnL^1Cl_2]$ and $[MnL^2Cl_2]$ are non-electrolytes, that is the solid state structures (Fig. 1) are conserved in solution; the iodo compounds $[MnL^1I_2]$ and $[MnL^2I_2]$ have solid state structures that are similar to those of the chloro compounds in Fig. 1, that is *cis*-octahedral (see solid state magnetic properties). In solution the iodo complexes are 1 : 1 electrolytes, that is one iodide is substituted by an acetonitrile donor (the electronic spectra suggest conservation of octahedral co-ordination geometry in solution). In the triflato complex $[MnL^1(O_3SCF_3)_2]$ both triflates are dissociated in solution, yielding a bis-(acetonitrile) species, that is a 2 : 1 electrolyte.

Acknowledgements

We are grateful to Dr Stefan Grutke for assistance with the thermogravimetric experiments and to BASF AG, Ludwigshafen, for financial support.

References

1 G. T. Babcock, *New Comprehensive Biochemistry-Photosynthesis*, ed. J. Amesz, Elsevier, New York, 1987.

2 J. J. R. Fraústo da Silva and R. J. P. Williams, *The Biological Chemistry of the Elements*, Clarendon Press, Oxford, 1991; J. Reedijk, *Bioinorganic Catalysis*, Marcel Dekker, New York, Basel, Hong Kong, 1993.

3 J. W. Whittaker and M. M. Whittaker, *J. Am. Chem. Soc.*, 1991, **113**, 5528.

4 W. C. Stallings, K. A. Pattridge, R. K. Strong and M. L. Ludwig, *J. Biol. Chem.*, 1985, **260**, 16424.

5 E. I. Du Pont De Nemours and Co., *Ger. Pat.* 1032526, 1956; Imperial Chemical Industries Limited (London), British Nylon Spinners Limited (Pontypool), *Ger. Pat.* 1172040, 1961.

6 J. Lemaire, J. L. Gardette, A. Rivaton and A. Roger, *Polym. Degrad. Stab.*, 1986, **15**, 1; V. Rossbach and T. Karstens, *Chemiefasern/Text. Ind.*, 1990, **40**, 603; D. Fromageot, A. Roger and J. Lemaire, *Angew. Makromol. Chem.*, 1989, **170**, 71.

7 P. R. Caujolle, A. Lattes, J. Jaud and J. Galy, *Acta Crystallogr., Sect. B*, 1981, **37**, 1699.

8 M. J. Fernandez, J. M. Casares and E. Calvez, *J. Heterocycl. Chem.*, 1992, **29**, 1797.

9 A. Samhammer, U. Holzgrabe and R. Haller, *Arch. Pharm.*, 1989, **322**, 545.

10 R. Caujolle, P. Castera and A. Lattes, *Bull. Chem. Soc. Fr.*, 1983, 413.

11 J. E. Douglass and T. B. Ratliff, *J. Org. Chem.*, 1968, **33**, 355.

12 G. M. Sheldrick, (a) SHELXS 86, University of Göttingen, 1986; (b) SHELXL 97, University of Göttingen, 1997.

13 G. M. Sheldrick, SHELXTL PLUS, Bruker Analytical X-ray Division, Madison, WI, 1995.

14 C. K. Johnson, ORTEP, A Thermal Ellipsoid Plotting Program, Oak Ridge National Laboratory, Oak Ridge, TN, 1965.

15 R. Haller, *Arch. Pharm.*, 1968, **301**, 741.

16 R. Haller, *Arch. Pharm.*, 1969, **302**, 113.

17 P. Comba, B. Nuber and A. Ramlow, *J. Chem. Soc., Dalton Trans.*, 1997, 347.

18 P. O. Lumme and E. Lindell, *Acta Crystallogr., Sect. C*, 1988, **44**, 463.

19 H. Börzel, P. Comba, C. Katsichtis, W. Kiefer, A. Lienke, V. Nagel and H. Pritzkow, *Angew. Chem.*, submitted.

20 K. R. Reddy and M. V. Rajasekharan, *Polyhedron*, 1994, **13**, 765.

21 F. Bohlmann, *Angew. Chem.*, 1957, **69**, 641; *Chem. Ber.*, 1958, **91**, 2157.

22 L. L. Martin, R. L. Martin, K. S. Murray and A. M. Sargeson, *Inorg. Chem.*, 1990, **29**, 1387.

Paper 8/05944F